Accepted Manuscript

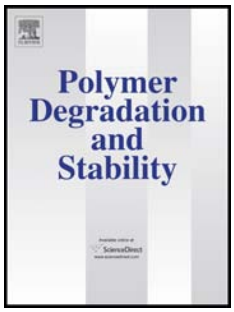

Influence of thymol and silver nanoparticles on the degradation of poly(lactic acid) based nanocomposites: thermal and morphological properties

Marina Ramos, Elena Fortunati, Mercedes Peltzer, Franco Dominici, Alfonso Jiménez, María del Carmen Garrigós, José María Kenny

PII: S0141-3910(14)00059-7

DOI: 10.1016/j.polymdegradstab.2014.02.011

Reference: PDST 7251

To appear in: *Polymer Degradation and Stability*

Received Date: 4 December 2013

Revised Date: 3 February 2014

Accepted Date: 10 February 2014

Please cite this article as: Ramos M, Fortunati E, Peltzer M, Dominici F, Jiménez A, Garrigós MdC, Kenny JM, Influence of thymol and silver nanoparticles on the degradation of poly(lactic acid) based nanocomposites: thermal and morphological properties, *Polymer Degradation and Stability* (2014), doi: 10.1016/j.polymdegradstab.2014.02.011.

Influence of thymol and silver nanoparticles on the degradation of poly(lactic acid) based nanocomposites: thermal and morphological properties

Marina Ramos[1*], Elena Fortunati[2], Mercedes Peltzer[1], Franco Dominici[2], Alfonso Jiménez[1], María del Carmen Garrigós[1], José María Kenny[2,3]

[1]Analytical Chemistry, Nutrition & Food Sciences Department, University of Alicante, Campus San Vicente del Raspeig, 03080, Alicante, Spain

[2]Materials Engineering Centre, UdR INSTM, University of Perugia, Str. Pentima 4, 05100 Terni, Italy

[3]Institute of Polymer Science and Technology, CSIC, Juan de la Cierva 3, 28006 Madrid, Spain

[*]Corresponding author. Marina Ramos. E-mail address: marina.ramos@ua.es

Tel.: +34 965903400 Ext. 3117; fax: +34 965903697.

Abstract

Biopolymers, such as poly(lactic acid) (PLA), have been proposed as environmentally-friendly alternatives in applications such as food packaging. In this work, silver nanoparticles and thymol were used as active additives in PLA matrices, combining the antibacterial activity of silver with the antioxidant performance of thymol. The combined action of both additives influenced PLA thermal degradation in ternary systems. DSC results showed that the addition of thymol resulted in a clear decrease of the glass transition temperature (T_g) of PLA, suggesting its plasticizing effect in PLA matrices. Slight modifications in mechanical properties of dog-bone bars were also observed after the addition of the active components, especially in the elastic modulus. FESEM analyses showed the good distribution of active additives through the PLA matrix, obtaining homogenous surfaces and highlighting the presence of silver

nanoparticles successfully embedded into the bulk matrix. Degradation of these PLA-based nanocomposites with thymol and silver nanoparticles in composting conditions indicated that the inherent biodegradable character of this biopolymer was improved after this modification. The obtained nanocomposites showed suitable properties to be used as biodegradable active-food packaging systems with antioxidant and antimicrobial effects.

Keywords: *Poly(lactic acid); Thymol; Silver nanoparticles; Nanocomposites; Degradation.*

1. Introduction

The use of biocompatible and biodegradable polymers has raised in the last years by their environmentally-friendly character and low dependence of non-renewable resources [1]. Among them, poly(lactic acid) (PLA) has received most attention due to its renewable nature, biodegradable character, biocompatibility and adequate mechanical and optical properties [2-3].

Within the last years, different technologies, in particular active packaging, have been proposed to improve the quality and shelf-life of food products [4-5]. Active compounds have different nature, such as oxygen, ethylene, water or odour scavengers [6-7], and antimicrobial or antioxidant compounds [8-9]. In this framework, essential oils extracted from plants or spices are rich sources of biological active compounds, such as terpenoids and phenolic acids [5]. In particular, thymol is present as one of the major compounds in thyme and oregano essential oils [10]. This is a phenolic monoterpene that has received considerable attention as an antimicrobial agent showing very high antifungal activity and antioxidant performance [11-12]. Different polymer

matrices, such as polypropylene (PP) and bio-based materials, such as caseinates, soy proteins and pectins have been proposed as adequate supporters for thymol in active systems [11, 13-14].

Silver nanoparticles (Ag-NPs) have been studied in different applications, including food packaging, due to their strong antibacterial properties [15-16]. Ag-NPs have high thermal stability and low volatility, and consequently their antimicrobial action could last longer [17-18]. Martinez-Abad et al prepared PLA films with 0.001-1.0 wt.% silver ions by the solvent casting technique demonstrating a good incorporation of the silver ions into the polymer matrix [19]. The PLA-silver composites showed strong *in vitro* antibacterial and antiviral activities, with increasing effect at higher silver concentrations. Fortunati et al. developed a nanobiocomposite based on PLA and combining silver nanoparticles with cellulose nanocrystals obtaining an antimicrobial film with enhanced barrier properties [20].

The effect of different additives on the PLA biodegradation has recently attracted great interest [21-23]. It is well known that PLA formulations require severe degradation conditions (as those provided by composting systems) to biodegrade in times compatible with useful post-use elimination strategies [24]. PLA is receiving considerable attention for single use applications, such as packaging, but also for more durable applications, such as car interior parts, textile fibres, flooring materials, among others [25]. Therefore, it is likely that the applications window of PLA will be greatly increased in the near future and degradation should be carefully studied to cope with potential widespread use of this polymer [26-27].

The aim of this work is the development and characterization of novel nanocomposites based on PLA, silver nanoparticles (Ag-NPs) and thymol. Moreover,

the evaluation of the influence of these active components on the composites degradation in composting conditions has been studied.

2. Experimental

2.1. Materials

A commercial poly(lactic acid) PLA-4060D (T_g = 58 ºC, 11-13 wt% D-isomer) was purchased in pellets from Natureworks Co., (Minnetonka, MN, USA). Commercial silver nanoparticles (Ag-NPs), P203, with a size distribution range from 20 to 80 nm, were purchased from Cima Nano-Tech (Saint Paul, MN, USA). Ag-NPs were thermally treated at 700 ºC for 1 h as reported elsewhere [28]. Thymol (99.5 %) was supplied by Sigma-Aldrich (Madrid, Spain).

2.2. Nanocomposites preparation

Nanocomposites were processed in a twin-screw microextruder (Dsm Explore 5&15 CC Micro Compounder, Heerlen, The Netherlands), with a temperature profile 170-180-190 ºC. PLA pellets were dried overnight at 45 ºC before extrusion to prevent PLA hydrolysis during processing. The screw speed was 150 rpm and a mixing time of 6 min was used to obtain the binary system, PLA-Ag-NPs 1 wt% (PLA/Ag). PLA and thymol binary systems were obtained by addition of 6 or 8 wt% to the polymer and these systems were named as PLA/T6 and PLA/T8, respectively. Thymol was added in the last three minutes of the extrusion and the screw speed was then reduced to 100 rpm to limit losses by vaporization.

Ternary systems with PLA and silver nanoparticles and thymol as additives were also prepared. A masterbatch of PLA and Ag-NPs was first processed in the extruder at

170-180-190 ºC temperature profile, screw speed 150 rpm and 3 min mixing time. This masterbatch was then combined with 6 or 8 wt% of thymol for 3 additional minutes to produce ternary formulations. Neat PLA with no additives was also processed in the same conditions and further used as control. After mixing, tensile dog-bone bars (ISO 527-2/5A) were prepared by means of a DSM Xplore 10-mL injection moulding machine. The injection pressure was set to 12.5 bars and the temperature maintained at 200 ºC. All materials used in this work are summarized in Table 1.

Table 1.

2.3. Nanocomposites characterization

2.3.1. Thermal characterization

Thermogravimetric analysis was performed to neat PLA and PLA nanocomposites with a TGA Seiko Exstar 6300 (USA). Approximately 8 mg samples were heated from 25 ºC to 700 ºC at 10 ºC min^{-1} heating rate under nitrogen atmosphere (flow rate 250 mL min^{-1}).

Differential scanning calorimetry (DSC) tests were conducted for the determination of glass transition temperatures (T_g) by using a DSC Mettler Toledo 822/e (Schwerzenbach, Switzerland) under nitrogen atmosphere (50 mL min^{-1}). 3 mg samples were introduced in aluminium pans (40 µL) and were submitted to the following thermal program: -25 ºC to 250 ºC at 10 ºC min^{-1}, with two heating and one cooling scans.

2.3.2. Mechanical properties

Tensile tests were used to evaluate the mechanical behaviour of neat PLA and PLA binary and ternary nanocomposites by using a digital Lloyd instrument LR 30K with a cross-head speed of 1 mm min^{-1} and a load cell of 30 kN. The dog-bone-shaped

specimens (2 mm thick) were prepared by following the procedures indicated in UNE ISO 527 Standard. Elongation at break (ε_b), tensile strength (σ_b) and elastic modulus (E_{young}) were calculated from the resulting stress-strain curves for all samples according to ASTM D882-09 Standard procedure [29]. Tests were carried out at room temperature and all values reported are the average of five measurements.

2.3.3. Field emission scanning electron microscopy (FESEM)

The surface of neat PLA and PLA nanocomposites and the cross section of PLA/Ag/T6 and PLA/Ag/T8 ternary formulations were analysed by field emission scanning electron microscopy (FESEM, Supra 25-Zeiss, Jena, Germany) to study their homogeneity and influence of thymol and Ag-NPs on the PLA morphology. Samples were coated with a gold layer prior to analysis in order to increase their electrical conductivity.

2.4. Disintegrability in composting conditions

Disintegration tests in composting conditions were performed by following the ISO 20200 Standard method using commercial compost with certain amount of sawdust, rabbit food, starch, oil and urea [30]. Tested samples were obtained from the previously prepared dog-bone bars, which were cut in pieces (15 x 5 x 2 mm^3), buried at 5 cm depth in perforated boxes and incubated at 58 ºC. The aerobic conditions were guaranteed by mixing the compost softly and by the periodical addition of water according to the standard requirements.

Different disintegration times were selected to recover samples from their burial and further tested: 0, 7, 14, 21, 28, 35 and 57 days. Samples were immediately washed with distilled water to remove traces of compost extracted from the container and further dried at 37 °C for 24 h before gravimetrical analysis. The disintegrability value for each

material at different times was obtained by normalizing the sample weight with the value obtained at the initial time.

The evolution of thermal properties upon disintegrability tests was studied by DSC from -25 to 250 ºC, at 10 ºC min^{-1}; and the morphological changes in the surface at 0 and 14 days of the incubation test was studied by FESEM. Fourier infrared spectra (Jasco FT-IR 615, USA) were recorded in the 400-4000 cm^{-1} range, in attenuated total reflection (ATR) mode. Finally, photographs of the samples were taken for visual evaluation.

3. Results and discussion

3.1. Nanocomposites thermal properties

The effect of the addition of thymol and Ag-NPs in the thermal stability of PLA-based nanocomposites was studied by TGA under nitrogen atmosphere. The weight loss (TG) and derivative DTG curves of binary and ternary systems are reported in Fig 1(a) and Fig 1(b), respectively. Table 2 shows the thermal parameters obtained from this study: initial degradation temperature (T_{ini}), determined at 5% weight loss, and maximum degradation temperature (T_{max}). All materials showed a main peak associated to the PLA thermal degradation between 330 and 360 ºC, as previously reported [31-33]. A slight reduction in T_{max} value was observed by the addition of Ag-NPs. On the other hand, a significant reduction in T_{ini} values was observed suggesting some loss in the PLA thermal stability. Meanwhile, thermograms of the PLA-thymol nanocomposites showed a first degradation step around 120 ºC, which could be related to the thymol degradation [11]. In summary, TGA results showed that besides the thermal stability of these nanocomposites was slightly reduced by the addition of

thymol and Ag-NPs, these formulations could be processed at the same temperature region (up to 200 ºC) than neat PLA without risking thermal degradation.

Fig. 1.

Table 2

DSC thermograms obtained for all samples and heating and cooling scans after processing are shown in Fig. 2. Since PLA used in this study is mostly amorphous, a clear glass transition temperature (T_g) for all samples could be determined (Table 2). Since this parameter is dependent upon the polymer structural arrangement and corresponds to the torsion oscillation of the carbon backbone [34], it was expectable that the addition of thymol could lead to some reduction in T_g, as observed in Table 2. In fact, binary and ternary systems with thymol showed a decrease in more than 10 °C on T_g values. This reduction is due to the plasticizing effect of thymol in polymer matrices [11], increasing the molecular mobility in the polymer structure. A similar behaviour was reported for the addition of other antioxidants to PLA with a remarkable reduction on T_g values [31, 35-36]. DSC results also showed that the addition of Ag-NPs had no relevant effect on the PLA T_g values, in agreement with previous studies [37]. On the other hand, parameters related to PLA nanocomposites crystallization or melting were not observed due to the amorphous structure of the polymer used in this study. No effects on polymer crystallization were noticeable after the addition of thymol and Ag-NPs.

Fig. 2

3.2. Nanocomposites morphology

Fig. 3 shows FESEM micrographs of neat PLA and PLA nanocomposites surfaces after processing and before the disintegration test in composting conditions. Homogeneous surface morphologies were observed for all materials, with no apparent effects of the thymol and Ag-NPs addition to the PLA matrix. FESEM micrographs were also taken to cross-section of ternary systems to evaluate the incorporation to the polymer matrix of both additives (Fig. 4). It was noticed that Ag-NPs were well dispersed with no apparent agglomerates, which could be probably related to the presence of thymol in these formulations [38].

Fig. 3

Fig. 4

3.3. Nanocomposites mechanical behaviour

The mechanical behaviour of neat PLA and nanocomposites was evaluated and results are reported in Table 2. The addition of 1 wt% of Ag-NPs to PLA had no significant effect on the elastic modulus, tensile strength and elongation at break values as already reported by Kanmani et al. [39]. Some reduction in tensile strength values was detected on PLA-thymol binary systems, being more evident for the highest content (8 wt%). This effect could be due to the increase in polymer chains mobility caused by the presence of thymol in these formulations [11, 40].

The combined action of thymol and Ag-NPs on the PLA mechanical behaviour was also evaluated. A slight decrease in tensile strength and elastic modulus of the ternary formulations was observed resulting in more flexible and stretchable materials. It could be suggested that the presence of Ag-NPs contributed to the thymol ability to increase the PLA chain mobility, which also promoted a more effective dispersion of silver

nanoparticles. These combined effects could be related to the presence of Van der Waals interactions between the hydroxyl groups of thymol molecules and the partial positive charge on the surface of the Ag-NPs which affects the mechanical response of the ternary nanocomposites [3, 40-41].

3.4. Degradation in compost

3.4.1. Visual analysis and disintegrability

The visual evaluation of all samples at different degradation times was carried out and results are shown in Fig. 5. Changes in samples surfaces after different times in contact submitted to composting conditions were clearly appreciable. All samples showed considerable modifications in colour and a general loss of transparency after 7 treatment days. These surface modifications were indicative of the beginning of the polymer hydrolytic degradation process, which was related to the moisture absorption. Fukushima et al. related the increase in the materials opacity to various simultaneous phenomena, such as the formation of low molar-mass degradation by-products during hydrolysis and/or the evolution in crystallinity in the polymer matrix [42]. Indeed, the general increase in the polymer and nanocomposites crystallinity took place at a higher rate in their amorphous zones [43]. This important cristallinity behaviour was expected and it was due to the already reported mostly amorphous character of the PLA used in this work and the large content in the D-LA enantiomer [44]. Further results at longer testing times showed that physical degradation progressed with burial time resulting in a complete loss of the initial morphology and general rupture after 35 days.

Fig. 5

Fig. 6(a) reports the disintegrability percentage as a function of the testing time for all materials. Before 14 days, no significant differences were observed between all samples with a general weight loss. However, after 14 days, those formulations containing thymol increased their weight loss rate and in consequence the disintegrability ratio to values higher than 30 %; while neat PLA and PLA/Ag showed slower degradation rate with values (20.8 ± 0.6) % and (24.4 ± 4.0) % after 21 days, respectively. These differences in disintegrability rate between those nanocomposites with and without thymol in their formulations increased after 35 days (Fig. 6(b)).

The PLA/Ag/T8 ternary nanocomposite showed the highest disintegration rate followed by PLA/Ag/T6 highlighting the high influence of thymol in the diffusion process of water molecules through the polymer structure, promoting hydrolysis, due to the increase in chain mobility induced by the combined presence of the additives, as previously discussed. This behaviour was improved by the homogeneous dispersion of thymol into the PLA matrix (as it was observed in FESEM micrographs). In addition, the thymol hydroxyl groups can contribute to the heterogeneous hydrolysis of the PLA matrix after absorbing water from the composting medium, resulting in noticeable increase in disintegrability values for PLA nanocomposites with thymol after 14 testing days. In the initial stages of the composting test, some interaction with formation of hydrogen bonds between the thymol hydroxyl groups and water molecules could retain the beginning of the hydrolysis process compensating the higher water diffusion rate in samples with thymol. However, after 14 days a clear increase in the disintegrability rate in the case of nanocomposites with thymol (binary and ternary systems) was observed in comparison with PLA and PLA/Ag. A similar behaviour was already reported by Sinha Ray et al., who suggested that 14 days could be considered the critical value to start the heterogeneous hydrolysis processes [45]. The presence of hydroxyl groups in

the thymol molecules, finely dispersed in the PLA matrix, are responsible of the formation of labile bonds in the PLA structure and consequently the hydrolysis under these conditions should be higher by the formation of low molar mass chains [45-46]. This effect could be even reinforced by synergies between Ag-NPs and thymol, since Ag atoms could catalyze the disintegration process [15].

Finally, after 57 days, it was observed that all PLA nanocomposites appeared totally disintegrated fully satisfying the ISO Standard requirements for a biodegradable material [30].

Fig. 6

3.4.2. Chemical analysis (FTIR)

Results obtained for PLA/Ag/T8 before and up to 21 days under composting conditions were analyzed by FTIR and spectra are reported in Fig. 7. The typical stretching band of the carbonyl group (-C=O) at 1750 cm^{-1} attributed to lactide and the -C-O- bond stretching band by the PLA -CH-O- group at 1180 cm^{-1} were identified in the spectra [3]. As previously discussed, the hydrolytic degradation took place during the initial phases of the composting treatment, where the high molar mass PLA chains were hydrolyzed to form low molar mass oligomers with plenty of available hydroxyl and carboxylic acid groups [24].

Fig. 7

FTIR spectra after 21 degradation days showed a considerable decrease in the intensity of the peaks related to the carbonyl group (-C=O) from lactide at 1750 cm^{-1} and the simultaneous appearance of a typical IR absorption, next to this band, corresponding to carbonyl groups of carboxylic acids formed by the hydrolytic scission

of the ester groups [47]. In addition, the band at 1230 cm^{-1} corresponding to -C-O- stretching practically disappeared in the spectra of samples after 7 treatment days [15]. However, these results did not reveal important differences between binary and ternary formulations regardless of the thymol concentration.

3.4.3. Morphological analysis (FESEM)

FESEM micrographs of the nanocomposites surfaces after 14 days of degradation test are shown in Fig. 3. Important differences in the samples surfaces after composting were obtained. Before the beginning of the burial test (day 0) all materials showed smooth and neat surfaces, but after 7 days, fractures appeared; in agreement with the important changes observed in the visual study. The formation of fractures and surface holes for all samples was clearly indicative of the beginning of the hydrolytic degradation process [42]. After 14 testing days, those formulations with thymol showed important fractures up to 2 µm in width (Fig. 3). It was observed that, in general terms, higher amounts of thymol resulted in more degraded materials submitted to composting conditions. This effect was particularly relevant for ternary nanocomposites. In fact, binary and ternary formulations containing 8 wt% of thymol (PLA/T8 and PLA/Ag/T8), showed highly irregular surfaces with holes. This observation could be related to the higher amount of thymol and the consequent ability to produce higher hydrolysis rates with formation and release of low molecular weight compounds, such as simple alcohols and/or CO_2. This transformation could be also related to the action of microorganisms, which are able to convert these low molecular weight structures into CO_2 and water [24].

3.4.4. Thermal analysis (DSC)

Fig. 8 shows the DSC thermograms obtained during the first heating scan for all formulations as a function of the composting time. It was observed that all nanocomposites were amorphous before the disintegration test, as expected from the amorphous characteristics of the PLA used in this study. In these thermograms, endothermic peaks corresponding to the enthalpic relaxation process were observed in all materials just after T_g. These peaks are indicative of the aging of the PLA before the beginning of the test, as it was reported in previous works [33-34]. However, the initially amorphous samples developed multiple endothermic peaks just after the seventh testing day. This observation was related to the formation of different crystalline structures with different perfection degrees in the PLA matrix during degradation, which was promoted by the hydrolysis process resulting in important changes in the materials crystallinity. Similar results were already reported by other authors, who suggested that the appearance of multiple melting peaks could be related to the formation of different crystal structures due to the polymer chains scission produced during the degradation process [15, 24, 44].

Fig. 8

DSC thermograms recorded during the second heating scan (data not shown) did not reveal crystallization and melting peaks, as it was expected. However, it was observed that the T_g values, calculated from the second heating scan, decreased with the testing time, upon 21 days of study (Fig. 9). This behaviour could be associated with the increase in the mobility of the polymer chains as a consequence of the hydrolytic process [33]. These new chains formed by lactic acid oligomers with low molar mass produced a plasticizing effect [44-46]. Nanocomposites with thymol showed a clear decrease in T_g between 7 and 14 testing days, suggesting that the formation of lactic

334 acid oligomers and the addition of thymol would increase the above-referred
335 plasticizing effect.

336 **Fig. 9**

337

338 **4. Conclusions**

339 Nanocomposites based on PLA, thymol and silver nanoparticles were developed and
340 fully characterized. The biodegradation properties under composting conditions were
341 also evaluated. The combination of the two additives influenced some of the matrix
342 properties, particularly thermal degradation. DSC results showed that the addition of
343 thymol resulted in a decrease in the glass transition temperature (T_g) of PLA, favouring
344 the plasticization of the polymer matrix. Slight modifications in tensile properties of
345 dog-bone bars obtained from all nanocomposites, especially in the elastic modulus
346 values, were attributed to the addition of both additives. FESEM micrographs showed
347 good distribution of the active additives through the PLA matrix, with homogenous
348 surfaces and highlighting the presence of silver nanoparticles successfully embedded
349 into the polymer matrix.

350 The degradation study of all nanocomposites in composting conditions showed that
351 the inherent biodegradable character of PLA was improved by the addition of thymol
352 and Ag-NPs, getting a faster degradation rate and meeting the biodegradation legal
353 requirements. These results suggest the potential of these nanocomposites as
354 environmentally-friendly active food packaging systems with an intrinsic biodegradable
355 nature.

356

Acknowledgements

Authors would like to thank Spanish Ministry of Economy and Competitiveness for financial support (MAT-2011-28468-C02-01). Moreover, Marina Ramos would like to thank University of Alicante (Spain) for UAFPU2011-48539721S predoctoral research grant.

References

[1] Alix S, Mahieu A, Terrie C, Soulestin J, Gerault E, Feuilloley MGJ, et al. Active pseudo-multilayered films from polycaprolactone and starch based matrix for food-packaging applications. Eur Polym J. 2013;49:1234-42.

[2] Urayama H, Kanamori T, Kimura Y. Properties and Biodegradability of Polymer Blends of Poly(L-lactide)s with Different Optical Purity of the Lactate Units. Macromol Mater Eng. 2002;287:116-21.

[3] Kamyar Shameli MBA, Wan Md Zin Wan Yunus, Nor Azowa Ibrahim, Russly Abdul Rahman, Maryam Jokar, Majid Darroudi. Silver/poly (lactic acid) nanocomposites: preparation, characterization, and antibacterial activity. Int J Nanomed. 2010;5:573-9.

[4] Vermeiren L, Devlieghere F, Van Beest M, De Kruijf N, Debevere J. Developments in the active packaging of foods. Trends Food Sci Tech. 1999;10:77-86.

[5] Bakkali F, Averbeck S, Averbeck D, Idaomar M. Biological effects of essential oils - A review. Food Chem Toxicol. 2008;46:446-75.

[6] Charles F, Sanchez J, Gontard N. Absorption kinetics of oxygen and carbon dioxide scavengers as part of active modified atmosphere packaging. J Food Eng. 2006;72:1-7.

[7] Rooney ML. Active packaging in polymer films. In: Rooney ML, editor. Active Food Packaging: Springer US; 1995. p. 74-110.

[8] Unalan lU, Arcan I, Korel F, Yemenicioglu A. Application of active zein-based films with controlled release properties to control Listeria monocytogenes growth and lipid oxidation in fresh Kashar cheese. Innov Food Sci Emerg. 2013 http://dx.doi.org/10.1016/j.ifset.2013.08.004.

384 [9] Camo J, Beltrán JA, Roncalés P. Extension of the display life of lamb with an antioxidant active
385 packaging. Meat Sci. 2008;80:1086-91.
386 [10] Al-Bandak G, Oreopoulou V. Antioxidant properties and composition of Majorana syriaca extracts.
387 Eur J Lipid Sci Tech. 2007;109:247-55.
388 [11] Ramos M, Jiménez A, Peltzer M, Garrigós MC. Characterization and antimicrobial activity studies
389 of polypropylene films with carvacrol and thymol for active packaging. J Food Eng. 2012;109:513-
390 9.
391 [12] Park H-Y, Kim S-J, Kim KM, You Y-S, Kim SY, Han J. Development of Antioxidant Packaging
392 Material by Applying Corn-Zein to LLDPE Film in Combination with Phenolic Compounds. J
393 Food Sci. 2012;77:E273-E9.
394 [13] Gutierrez L, Batlle R, Sanchez C, Nerin C. New approach to study the mechanism of antimicrobial
395 protection of an active packaging. Foodborne Pathog Dis. 2010;7:1063-9.
396 [14] Sung S-Y, Sin LT, Tee T-T, Bee S-T, Rahmat AR, Rahman WAWA, et al. Antimicrobial agents for
397 food packaging applications. Trends Food Sci Tech. 2013;33:110-23.
398 [15] Fortunati E, Armentano I, Iannoni A, Barbale M, Zaccheo S, Scavone M, et al. New multifunctional
399 poly(lactide acid) composites: Mechanical, antibacterial, and degradation properties. J Appl Polym
400 Sci. 2012;124:87-98.
401 [16] Busolo MA, Fernandez P, Ocio MJ, Lagaron JM. Novel silver-based nanoclay as an antimicrobial in
402 polylactic acid food packaging coatings. Food Addit Contam A. 2010;27:1617-26.
403 [17] Cushen M, Kerry J, Morris M, Cruz-Romero M, Cummins E. Migration and exposure assessment of
404 silver from a PVC nanocomposite. Food Chem. 2013;139:389-97.
405 [18] Kumar R, Münstedt H. Silver ion release from antimicrobial polyamide/silver composites.
406 Biomaterials. 2005;26:2081-8.
407 [19] Martínez-Abad A, Ocio MJ, Lagarón JM, Sánchez G. Evaluation of silver-infused polylactide films
408 for inactivation of Salmonella and feline calicivirus in vitro and on fresh-cut vegetables. Int J Food
409 Microbiol. 2013;162:89-94.
410 [20] Fortunati E, Peltzer M, Armentano I, Jiménez A, Kenny JM. Combined effects of cellulose
411 nanocrystals and silver nanoparticles on the barrier and migration properties of PLA nano-
412 biocomposites. J Food Eng. 2013;118:117-24.

[21] Russias J, Saiz E, Nalla RK, Gryn K, Ritchie RO, Tomsia AP. Fabrication and mechanical properties of PLA/HA composites : A study of in vitro degradation. Mat Sci Eng C. 2006;26:1289–95.

[22] Rinaldi S, Fortunati E, Taddei M, Kenny JM, Armentano I, Latterini L. Integrated PLGA–Ag nanocomposite systems to control the degradation rate and antibacterial properties. J Appl Polym Sci. 2013;130:1185-93.

[23] Bitinis N, Fortunati E, Verdejo R, Bras J, Kenny JM, Torre L, et al. Poly(lactic acid)/natural rubber/cellulose nanocrystal bionanocomposites. Part II: Properties evaluation. Carbohyd Polym. 2013;96:621-7.

[24] Fukushima K, Abbate C, Tabuani D, Gennari M, Camino G. Biodegradation of poly(lactic acid) and its nanocomposites. Polym Degrad Stabil. 2009;94:1646-55.

[25] Armentano I, Bitinis N, Fortunati E, Mattioli S, Rescignano N, Verdejo R, et al. Multifunctional nanostructured PLA materials for packaging and tissue engineering. Prog Polym Sci. 2013;38:1720-47.

[26] Jeon HJ, Kim MN. Biodegradation of poly(l-lactide) (PLA) exposed to UV irradiation by a mesophilic bacterium. Int Biodeter Biodegr. 2013;85:289-93.

[27] Sangwan P, Wu DY. New Insights into Polylactide Biodegradation from Molecular Ecological Techniques. Macromol Biosci. 2008;8:304-15.

[28] Fortunati E, Armentano I, Iannoni A, Kenny JM. Development and thermal behaviour of ternary PLA matrix composites. Polym Degrad Stabil. 2010;95:2200-6.

[29] ASTM. D 882 - 09. Standard test method for tensile properties of thin plastic sheeting In: Annual book of ASTM standards Amer Soc for Testing & Materials, Philadelphia, PA2009.

[30] UNE-EN. ISO 20200:2006. Plastics - Determination of the degree of disintegration of plastic materials under simulated composting conditions in a laboratory-scale test (ISO 20200:2004). 2006.

[31] Hwang SW, Shim JK, Selke SEM, Soto-Valdez H, Matuana L, Rubino M, et al. Poly(L-lactic acid) with added α-tocopherol and resveratrol: optical, physical, thermal and mechanical properties. Polym Int. 2012;61:418-25.

[32] Martino VP, Jiménez A, Ruseckaite RA, Avérous L. Structure and properties of clay nano-biocomposites based on poly(lactic acid) plasticized with polyadipates. Polym Adv Technol. 2010;22:2206-13.

442 [33] Burgos N, Martino VP, Jiménez A. Characterization and ageing study of poly(lactic acid) films
443 plasticized with oligomeric lactic acid. Polym Degrad Stabil. 2013;98:651-8.
444 [34] Hughes J, Thomas R, Byun Y, Whiteside S. Improved flexibility of thermally stable poly-lactic acid
445 (PLA). Carbohyd Polym. 2012;88:165-72.
446 [35] Byun Y, Kim YT, Whiteside S. Characterization of an antioxidant polylactic acid (PLA) film
447 prepared with α-tocopherol, BHT and polyethylene glycol using film cast extruder. J Food Eng.
448 2010;100:239-44.
449 [36] Arrieta MP, López J, Ferrándiz S, Peltzer MA. Characterization of PLA-limonene blends for food
450 packaging applications. Polym Test. 2013;32:760-8.
451 [37] Fortunati E, Armentano I, Zhou Q, Iannoni A, Saino E, Visai L, et al. Multifunctional
452 bionanocomposite films of poly(lactic acid), cellulose nanocrystals and silver nanoparticles.
453 Carbohyd Polym. 2012;87:1596-605.
454 [38] Fortunati E, Armentano I, Zhou Q, Puglia D, Terenzi A, Berglund LA, et al. Microstructure and
455 nonisothermal cold crystallization of PLA composites based on silver nanoparticles and
456 nanocrystalline cellulose. Polym Degrad Stabil. 2012;97:2027-36.
457 [39] Kanmani P, Rhim J-W. Physical, mechanical and antimicrobial properties of gelatin based active
458 nanocomposite films containing AgNPs and nanoclay. Food Hydrocolloid. 2014;35:644-52.
459 [40] Fabra MJ, Talens P, Chiralt A. Tensile properties and water vapor permeability of sodium caseinate
460 films containing oleic acid–beeswax mixtures. J Food Eng. 2008;85:393-400.
461 [41] Aguirre A, Borneo R, León AE. Antimicrobial, mechanical and barrier properties of triticale protein
462 films incorporated with oregano essential oil. Food Biosci. 2013;1:2-9.
463 [42] Fukushima K, Tabuani D, Arena M, Gennari M, Camino G. Effect of clay type and loading on
464 thermal, mechanical properties and biodegradation of poly(lactic acid) nanocomposites. React
465 Funct Polym. 2013;73:540-9.
466 [43] Paul MA, Delcourt C, Alexandre M, Degée P, Monteverde F, Dubois P. Polylactide/montmorillonite
467 nanocomposites: study of the hydrolytic degradation. Polym Degrad Stabil. 2005;87:535-42.
468 [44] Gorrasi G, Pantani R. Effect of PLA grades and morphologies on hydrolytic degradation at
469 composting temperature: Assessment of structural modification and kinetic parameters. Polym
470 Degrad Stabil. 2013;98:1006-14.

[45] Sinha Ray S, Yamada K, Okamoto M, Ueda K. New polylactide-layered silicate nanocomposites. 2. Concurrent improvements of material properties, biodegradability and melt rheology. Polymer. 2003;44:857-66.

[46] Proikakis CS, Mamouzelos NJ, Tarantili PA, Andreopoulos AG. Swelling and hydrolytic degradation of poly(d,l-lactic acid) in aqueous solutions. Polym Degrad Stabil. 2006;91:614-9.

[47] Fukushima K, Feijoo JL, Yang M-C. Abiotic degradation of poly(dl-lactide), poly(ε-caprolactone) and their blends. Polym Degrad Stabil. 2012;97:2347-55.

480 **Figure Captions.**

481 **Fig. 1**. TG (a) and DTG (b) curves of neat PLA and binary and ternary systems with
482 Ag-NPs and thymol.

483 **Fig. 2.** DSC thermograms for PLA, PLA/Ag, PLA/T8 and PLA/Ag/T8 for the first
484 heating and cooling scans (a) and the second heating scan (b).

485 **Fig. 3.** FESEM micrographs of the surface of nanocomposites before (0 days) and after
486 14 days of disintegration in compost at 58 ºC (500x) and after 14 days with higher zoom
487 (10.00 kx).

488 **Fig. 4.** Cross section micrographs of PLA/Ag/T6 and PLA/Ag/T8 after processing.

489 **Fig. 5.** PLA and PLA nanocomposites before (0 days) and after different times under
490 composting conditions at 58ºC.

491 **Fig. 6.** Disintegrability (%) of PLA and PLA nanocomposites before (0 days) and after
492 different times in compost at 58 ºC. The line at 90 % represents the goal of
493 disintegrability test as required by the ISO 20200 Standard.

494 **Fig. 7.** FTIR spectra of PLA/Ag/T8 before (0 days) and after different times under
495 composting conditions.

496 **Fig. 8.** DSC thermograms obtained for all materials before (0 days) and after different
497 times under composting conditions at 58 ºC during the first heating scan (10 ºC min^{-1}).

498 **Fig. 9.** T_g values for all materials before (0 days) and after 21 days of disintegration
499 under composting conditions at 58 ºC during the second heating scan.

500

501 **Table. 1.** PLA nanocomposites formulated in this study.
502

Materials	PLA (wt%)	Ag-NPs (wt%)	Thymol (wt%)
PLA	100	-	-
PLA/Ag	99	1	-
PLA/T6	94	-	6
PLA/T8	92	-	8
PLA/Ag/T6	93	1	6
PLA/Ag/T8	91	1	8

503

504

505 **Table 2.** Thermal parameters and tensile properties of neat PLA and nanocomposites

506 after processing.

Samples	T_g[a] (ºC)	T_i[b] (ºC)	T_{max}[b] (ºC)	E_{young}[c] (MPa)	ε_b[c] (%)	σ_b[c] (MPa)
PLA	56 ± 3	324 ± 12	363 ± 6	3181 ± 35	3.5 ± 0.2	60.3 ± 8.0
PLA/Ag	56 ± 1	317 ± 8	357 ± 13	3000 ± 172	3.6 ± 0.2	59.7 ± 2.9
PLA/T6	50 ± 2	327 ± 15	358 ± 7	3289 ± 28	2.7 ± 0.2	52.1 ± 1.3
PLA/T8	42 ± 1	316 ± 14	353 ± 9	2930 ± 76	2.6 ± 0.3	36.4 ± 3.2
PLA/Ag/T6	44 ± 1	284 ± 9	337 ± 12	2823 ± 121	3.6 ± 0.3	36.9 ± 3.0
PLA/Ag/T8	41 ± 1	288 ± 5	336 ± 14	2547 ± 244	2.8 ± 0.2	36.3 ± 2.8

[a, b] (n=3; m ± SD)

[a] DSC data determined from the first heating scan at 10 ºC min^{-1}

[b] Determined by TGA analysis at 10 ºC min^{-1} in N_2 atmosphere. Corresponding with 2nd degradation step

[c] (n=5 ; m ± SD)

507

508

509

Figure 1 (a)

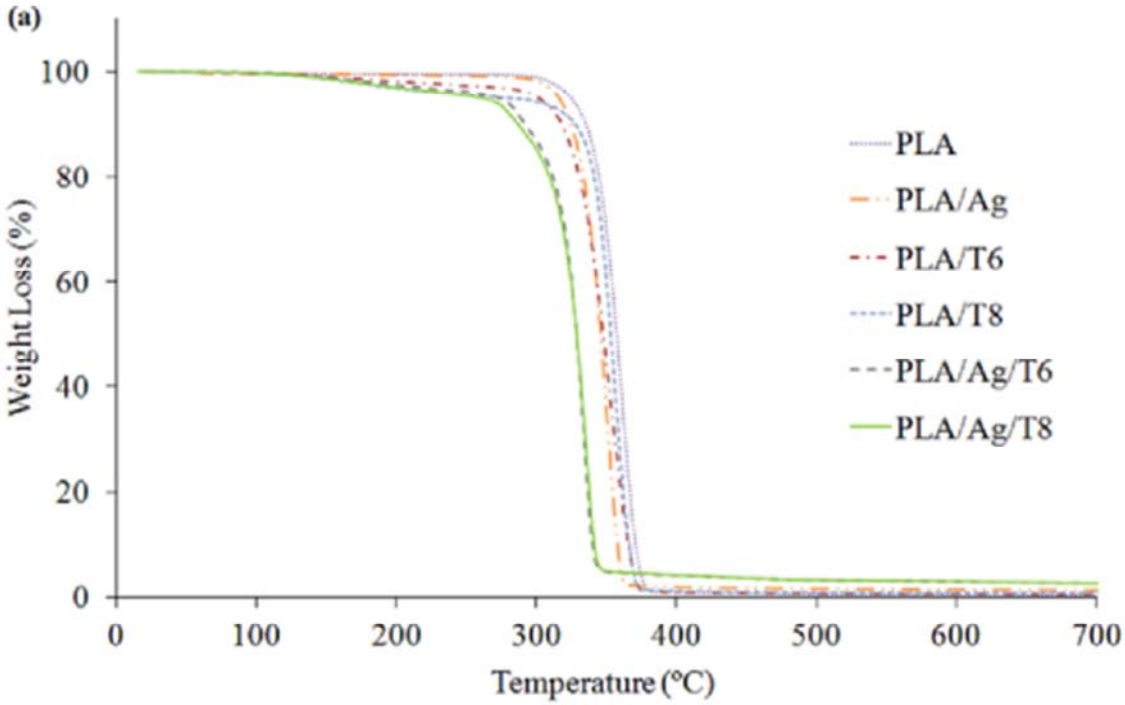

Figure 1 (b)

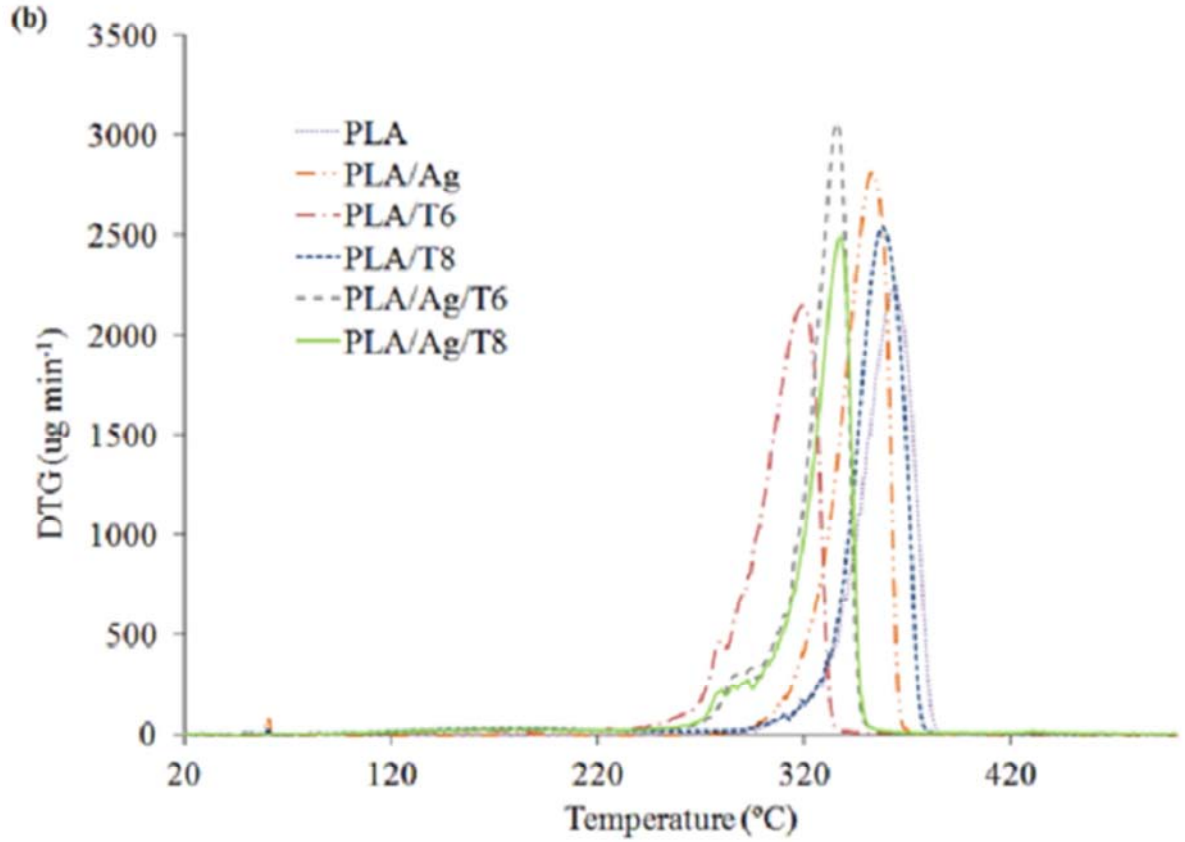

Figure 2(a)

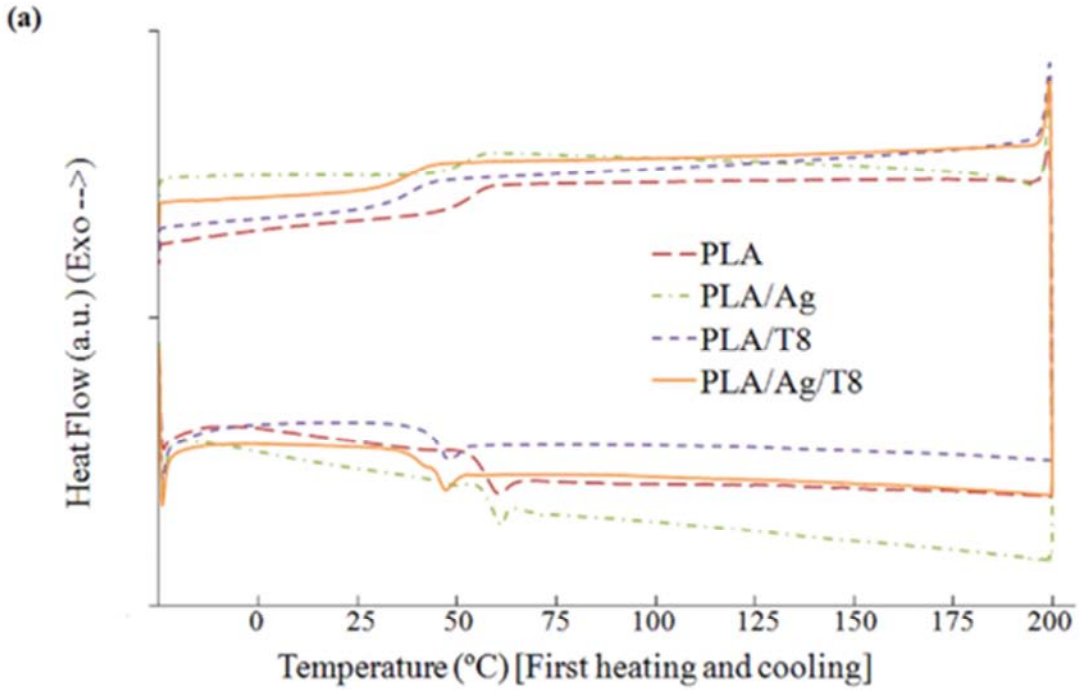

Figure 2 (b)

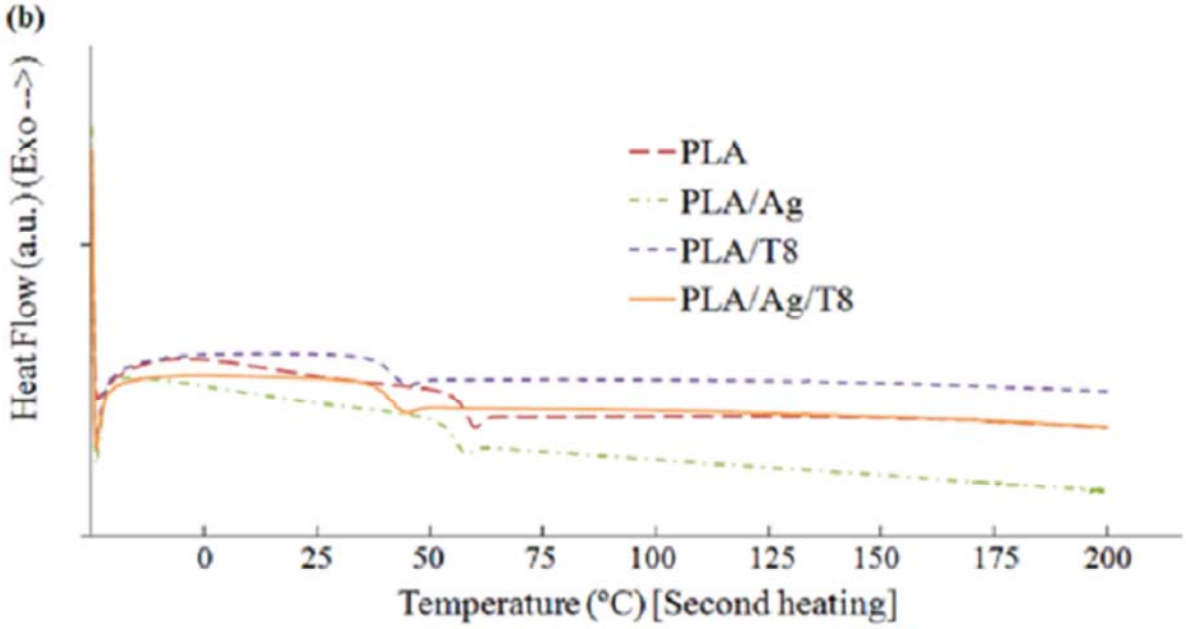

Modified Figure 3

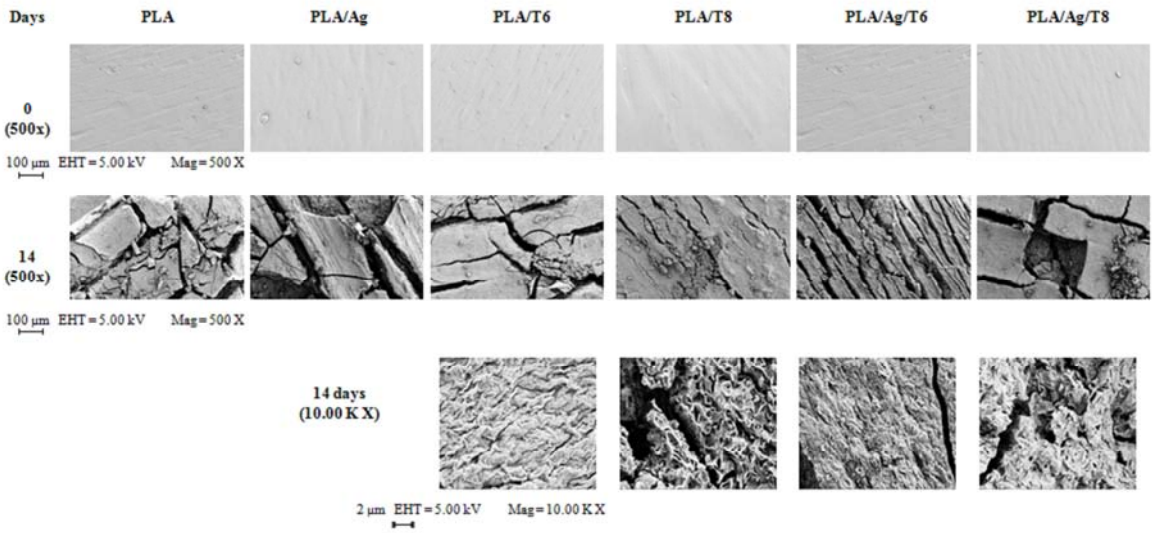

Figure 4

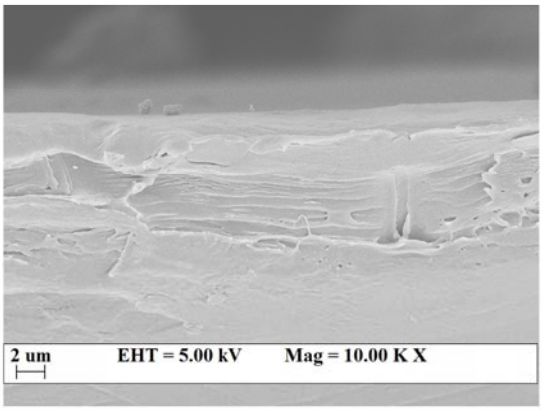

PLA/Ag/T6

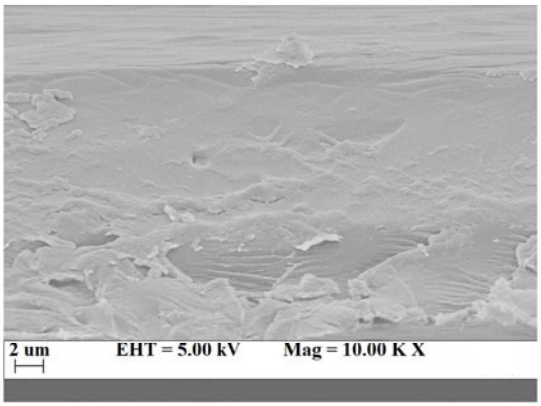

PLA/Ag/T8

Figure 5

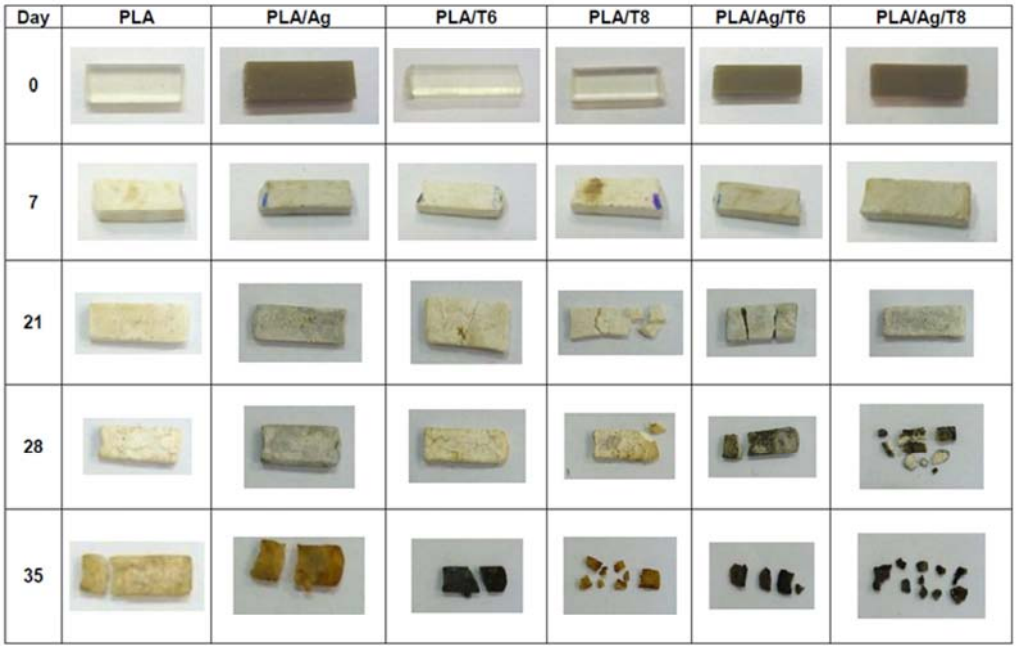

Figure 6

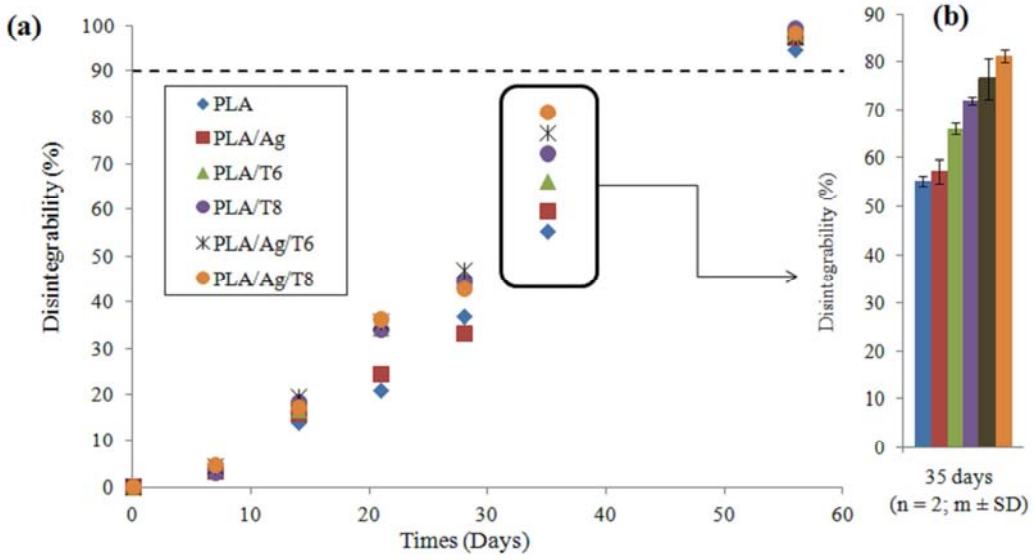

Modified Figure 7

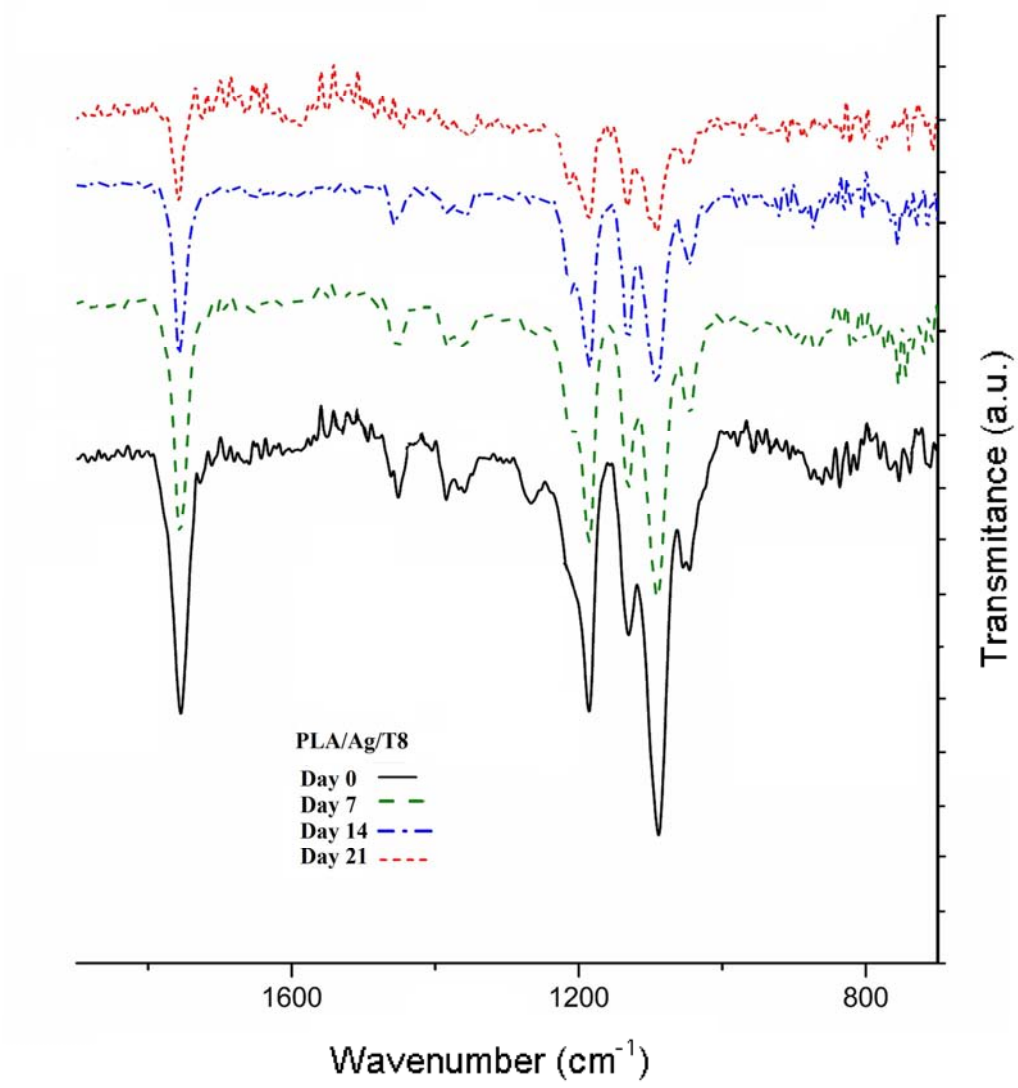

Modified Figure 8

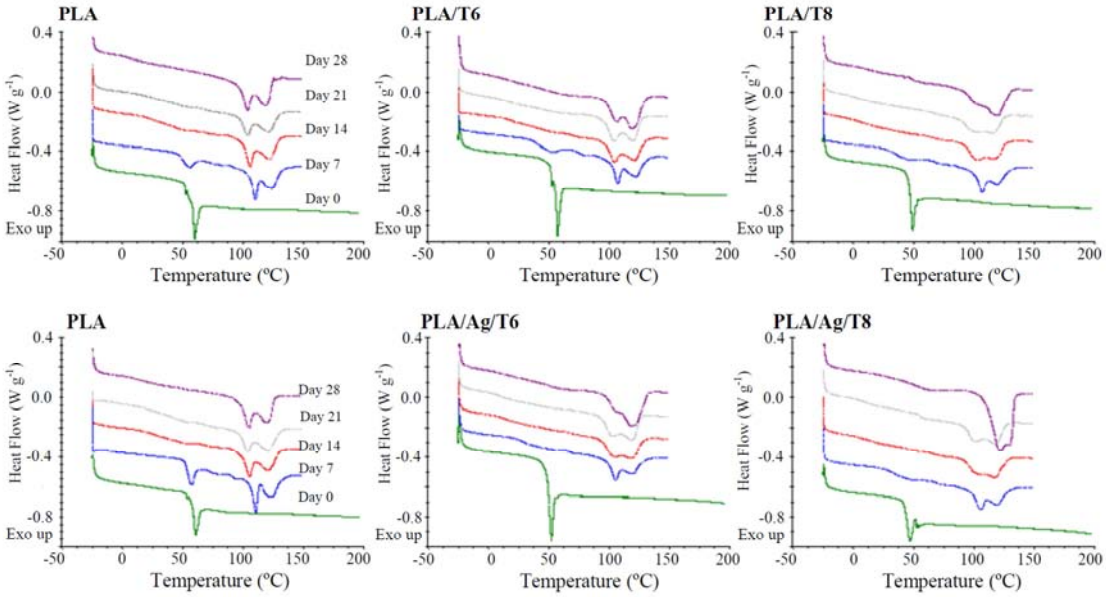

Figure 9